ChemComm

COMMUNICATION

View Article Online
View Journal | View Issue

Open Access Article. Published on 31 July 2015. Downloaded on 11/9/2025 4:47:51 AM.
This article is licensed under a Creative Commons Attribution-NonCommercial 3.0 Unported Licence.

Cite this: *Chem. Commun.*, 2015, **51**, 14187

Received 18th June 2015,
Accepted 29th July 2015

DOI: 10.1039/c5cc04999g

www.rsc.org/chemcomm

# $CO_2$-selective PEO–PBT (PolyActive™)/graphene oxide composite membranes†

M. Karunakaran, R. Shevate, M. Kumar and K.-V. Peinemann*

**$CO_2$-selective graphene oxide (GO) nano-composite membranes were prepared for the first time by embedding GO into a commercially available poly(ethylene oxide)–poly(butylene terephthalate) (PEO–PBT) copolymer (PolyActive™). The as-prepared GO membrane shows high $CO_2$ permeability (143 Barrer) and $CO_2/N_2$ selectivity ($\alpha$ = 73).**

Graphene based membranes have been considered to be promising membrane materials for separation applications.[1–5] The two-dimensional graphene is intrinsically impermeable to gas molecules; however, a derivative of graphene (GO) having a variety of functional groups shows significant potential in membrane separation applications.[6–10] Besides gas separation other applications like dehydration by pervaporation[11] and proton conduction with chemically modified free-standing GO films have been proposed.[12] The GO can be easily obtained by chemical oxidation of two-dimensional graphite using oxidizing agents. Polar oxygenated graphene (GO) forms stable dispersions in water and can be assembled into thin films.[7] GO films can be prepared using spin-coating, interfacial stitching, vacuum filtration, and direct evaporation methods.[13–16] Recently, high-performance GO membranes have been developed by filtering/spin coating of GO solution onto a porous support membrane.[1,3] It should be noted, however, that some of the published data should be considered with care. Kim *et al.* reported in *Science*[1] and later in *Chemical Communications*[13] a $CO_2$-permeability of more than 8000 Barrer combined with a $CO_2/N_2$-selectivity of 20. This extraordinarily high permeability is based on a miscalculation. Taking the permeances and thickness of the GO-composite membrane a $CO_2$-permeability smaller 1 Barrer is found to be the correct result (see ESI†). Nevertheless, the fabricated GO membranes showed high gas permeances. However, engineering GO membranes on the commercial scale by the aforementioned techniques will be a challenge. Free-standing thin GO membranes are brittle, and a thick layered graphene membrane cannot be used in a practical application process. Also, the different fabrication process would lead to GO membranes having different GO laminates and separation properties.[1–3,8,13]

On the other hand, polymer based gas separation membranes have emerged as an ideal candidate for use in large scale industrial separation applications. However, polymer based membranes have as a major drawback, the so-called permeability–selectivity trade off, *i.e.*, either increase in permeability or decrease in selectivity or *vice versa*.[17] In order to improve the membrane permeability, selectivity and stability for practical industrial applications the development of innovative membranes are required with process efficiency for industrial applications. To address this issue, various porous solid materials have been used as fillers, including zeolites, metal–organic frameworks, carbons, and silica.[18–20] Recently, GO nanosheets have been incorporated into polymer solutions to obtain selective transport channels for gas separation.[21,22] Since GO disperses excellently in aqueous media, most of the membranes were prepared using an aqueous solution. To disperse GO nanosheets into a polymer solution, the polymer should be soluble in an aqueous solution or in a water miscible solvent.

Here, we have succeeded in incorporating GO into a commercially available PEO–PBT copolymer (PolyActive™, PolyVation, NL) for membrane fabrication. PolyActive™ is a promising polymer for manufacturing $CO_2$-selective membranes. It has recently been fabricated into pilot scale modules for $CO_2$/hydrocarbon separation.[23] The copolymer contains 77 wt% of PEO (1500 g mol$^{-1}$) and 23 wt% of PBT, which possess O–C═O and C–O–C groups in the polymer backbone (Fig. S1, ESI†) and the copolymer is soluble in tetrahydrofuran (THF).[24] The advantage of the dissolution of PEO–PBT in THF is the miscibility with water. This allowed us to mix an aqueous GO-dispersion with the polymer solution without any phase separation or precipitation of the polymer during GO addition.

Membranes with various concentrations of GO (0.025%, 0.05%, 0.065%, 0.075%, 0.125%, 0.25, and 0.5%) were fabricated

*Advanced Membranes and Porous Materials Center, 4700 King Abdullah University of Science and Technology (KAUST), Thuwal 23955-6900, Kingdom of Saudi Arabia. E-mail: klausviktor.peinemann@kaust.edu.sa*

† Electronic supplementary information (ESI) available. See DOI: 10.1039/c5cc04999g

Open Access Article. Published on 31 July 2015. Downloaded on 11/9/2025 4:47:51 AM.
This article is licensed under a Creative Commons Attribution-NonCommercial 3.0 Unported Licence.

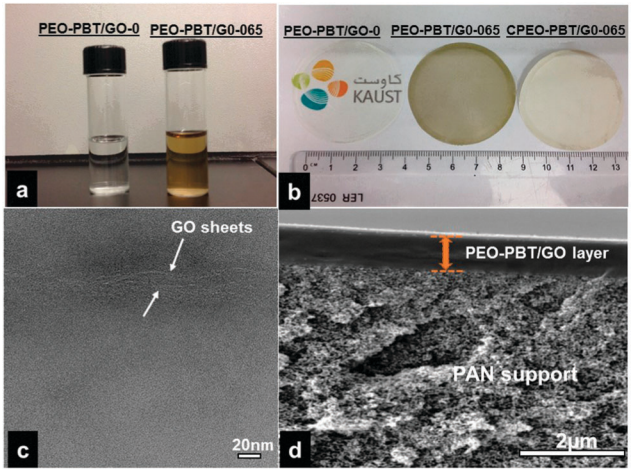


Fig. 1 (a) Digital photographs of PEO–PBT/GO-0 and PEO–PBT/GO-065 solution dispersed in THF/DI water (80/20 w/w), (b) digital images of free-standing PEO–PBT/GO-0, PEO–PBT/GO-065 dense and C-PEO–PBT/GO-065 composite membranes, (c) TEM image of PEO–PBT/GO-065 membrane cross-section, (d) cross-sectional SEM images of C-PEO–PBT/GO-065 composite membrane.

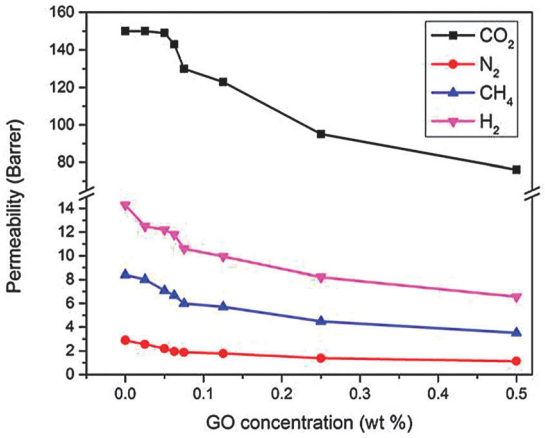


Fig. 2 Gas permeability of PEO–PBT/GO membranes as a function of various GO concentrations.

and denoted as PEO–PBT/GO-025, PEO–PBT/GO-050, PEO–PBT/GO-065, PEO–PBT/GO-075, PEO–PBT/GO-125, PEO–PBT/GO-250, and PEO–PBT/GO-500, respectively. Fig. 1a shows the photo-images of pure polymer solution and GO dispersed in PEO–PBT copolymer solution. The GO containing polymer solutions showed a very good dispersion of GO in THF/DI water 80 : 20 (w/w) mixture after sonication for 3 h. The GO nanosheets are heavily decorated by oxygen containing functional groups (hydroxyl, epoxide and carboxyl), which are responsible for hydrogen bonding interactions between GO–GO nanosheets and GO-polymer.[25] Fig. S2 (ESI†) shows the ATR-FTIR spectra for pure polymer and GO containing polymer membranes. The bands at 2874 $cm^{-1}$ ($-CH_2$), 1714 $cm^{-1}$ (–C═O), 1102 $cm^{-1}$ (C–O–C) and 726 $cm^{-1}$ (aromatic ring) represent the PEO–PBT polymer. Further discussion of the ATR-FTIR spectra can be found in the ESI.† Using the stable PEO–PBT/GO suspension, about 60 μm thick dense membranes were prepared by evaporating the solvent at room temperature from a Teflon Petri dish. Fig. 1b shows the digital photograph images of the pristine PEO–PBT membrane, the PEO–PBT/GO dense membrane and the thin film composite membrane fabricated on a polyacrylonitrile (PAN) support. The TEM image of the PEO–PBT/GO-065 membrane in Fig. 1c also confirms the good dispersion of GO nanosheets in the membrane matrix. Fig. S3 (ESI†) shows the Raman spectra of GO, pure PEO–PBT and PEO–PBT/GO membranes. The two well-known G and D bands were obtained for the synthesized GO nanosheets, which are characteristic of carbon materials. The G band located at ~1580 $cm^{-1}$ corresponds to the vibration of $sp^2$-hybridized carbon. The D band located at ~1339 $cm^{-1}$ is due to the structural defects or reduced size of $sp^2$ domains. The intensity of the D band is related to the size of in-plane $sp^2$ domains.[26] Therefore, the intensity ratio of the D to the G band ($I_D/I_G$ ratio) is usually considered as an indication for the relative disorder in the structure of the graphene sheets. Further discussion of the Raman spectra can be found in the ESI.† PEO–PBT membranes with various concentrations of GO nanosheets were prepared and single gas permeation measurements were performed for the dense membranes. Fig. S4 (ESI†) shows the constant volume/variable pressure apparatus for gas permeability measurements. Fig. 2 shows the gas permeability data for various GO containing PEO–PBT membranes and the permeability values are expressed in terms of Barrer (1 Barrer = $1 \times 10^{-10}$ $cm^3$(STP) cm $cm^{-2}$ $s^{-1}$ $cmHg^{-1}$).

The $CO_2$ permeability of the pristine PEO–PBT membrane is 150 Barrer. Up to 0.05 wt% GO in the membrane the $CO_2$ permeability remained nearly a constant. The addition of more than 0.05% GO to PEO–PBT continuously decreased the $CO_2$ permeability (Table S1, ESI†). These results are in contrast to the results obtained with Pebax/GO mixed matrix membranes reported by Shen *et al.*[21] It was shown that the pure Pebax membrane has 70 Barrer of $CO_2$ permeability and upon addition of 0.1 wt% of GO to the Pebax membrane, the $CO_2$ permeability increased from 70 Barrer to 100 Barrer. Further addition of GO from 0.1 to 0.5 wt% led to a decrease of the $CO_2$ permeability from 100 to 30 Barrer.

In our case the $CO_2$ permeability of the PEO–PBT/GO mixed matrix membrane initially showed a $CO_2$ permeability similar to the pristine PEO–PBT membrane. The $CO_2$ permeability of PEO–PBT/GO membranes decreased from 150 Barrer to 76 Barrer with an increase in the GO concentration from 0.05 to 0.5 wt% loadings. Moreover, the incorporation GO to the PEO/PBT membrane showed a decrease in gas permeability for other gases such as $N_2$, $H_2$ and $CH_4$. From Fig. 3 it can been seen that the $CO_2/N_2$ selectivity increased from 52 to 73 with an increase of the GO nanosheet concentration up to 0.0625%. This reveals that a small incorporation of GO nanosheets in the PEO–PBT membrane increases the $CO_2/N_2$ selectivity and a further increase in the GO nanosheet concentration maintains the $CO_2/N_2$ selectivity ($\alpha = 70$) with decreasing gas permeability. The $CO_2/CH_4$ selectivity for the GO containing membrane was 21, which is higher than that of the pristine PEO–PBT membrane ($\alpha = 17$). Even at a high loading of GO nanosheets (0.5 wt%) the $CO_2/CH_4$ gas selectivity did not change and the selectivity was maintained at 21 with decrease

Open Access Article. Published on 31 July 2015. Downloaded on 11/9/2025 4:47:51 AM.
This article is licensed under a Creative Commons Attribution-NonCommercial 3.0 Unported Licence.

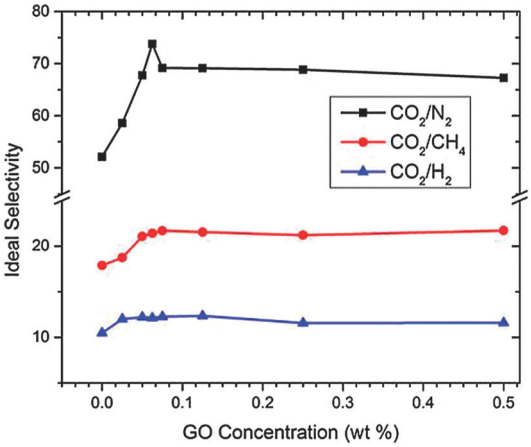


Fig. 3 Ideal gas selectivity of PEO–PBT/GO membranes as a function of various GO concentrations.

in permeability of both gases ($CO_2$ and $CH_4$). However, the interesting fact is that at about 0.065% loading of GO the mixed matrix membrane showed a $CO_2/N_2$ selectivity of 73 and a $CO_2$ permeability of 143 Barrer. By incorporating these data in the 2008 Robeson plot (Fig. 4), the gas permeability data surpass the upper bound curve at very low loadings of GO. Kim *et al.*[13] reported the high permeance of gases for an ultrathin GO coated polymer support membrane and the permeance order of gases through the GO membranes was $CO_2 > H_2 > CH_4 > O_2 > N_2$. This permeance is not following the kinetic diameter of gases ($CH_4 > N_2 > O_2 > CO_2 > H_2$), revealing that the permeance of the gases are not based on the size sieving of gas molecules by GO nanosheets. In addition, Shen *et al.*[21] reported that GO containing Pebax membranes allowed fastest transport of $CO_2$ and very low permeation of other gases. The gas permeability order of GO embedded Pebax membranes were $CO_2 > H_2 > CH_4 > N_2$. Moreover, the $CO_2$ permeability and selectivity of membranes are significantly enhanced with the increasing amount of GO nanosheets. In this study, the gas permeability order of the PEO–PBT/GO membrane was $CO_2 > H_2 > CH_4 > N_2$, which is similar to the gas permeability order reported by Kim[13] and Shen *et al.*[21] We noted in this study that the gas permeability of the PEO–PBT membrane also had the same permeability order as the pure GO membrane[13] (Fig. S5, ESI†). It has been reported that the gas adsorption of GO followed the order of $CO_2 > CH_4 > N_2 > H_2$.[3] The high $CO_2$ sorption capability of GO nanosheets is the main reason for the high $CO_2$ permeance. The permeability of a gas through the separation membranes is a product of gas diffusivity and solubility. Based on the solution-diffusion model the selectivity of the membranes can be expressed as:

$$\alpha = \frac{P_{CO_2}}{P_{N_2}} = \frac{D_{CO_2}}{D_{N_2}} \times \frac{S_{CO_2}}{S_{N_2}} \quad (1)$$

where $D$ is the gas diffusion coefficient and $S$ is the gas solubility coefficient. In the case of PEO–PBT/GO membranes, the $CO_2$ permeability was not enhanced after the addition of GO, but the $N_2$ permeability decreased and this led to the increase in $CO_2/N_2$ selectivity. The permeability of other gases such as $H_2$ and $CH_4$ also decreased with increasing GO content. The GO nanosheets hinder the diffusion of the other gases $N_2$, $H_2$ and $CH_4$, which leads to an increase in $CO_2/N_2$, $CO_2/H_2$ and $CO_2/CH_4$ selectivity. Since GO has a strong affinity for $CO_2$, we anticipated that the increase in the GO concentration would lead to an increase in $CO_2$ permeability. In the GO embedded PEO–PBT membranes the molecular transport occurs through the polymer matrix and the interlayer spacing of GO nanosheets. The stacking of GO nanosheets in the polymer matrix plays a crucial role in the fast molecular transport. Based on our understanding of achieving high molecular transport, the GO nanosheets should be uniformly dispersed in the polymer matrix. We assume a random orientation of the nanosheets in the polymer matrix. Fig. 5 shows schematically the two extreme possible orientations of GO nanosheets in the polymer matrix and the pathways for gas diffusions.

The GO nanosheets can be oriented perpendicular and parallel to the membrane surface. The diffusion of gas molecules through perpendicular GO nanosheets passes through the interlayer spacing of GO nanosheets and is then hindered by other GO nanosheets oriented parallel to the membrane surface. The hindrance by the parallel oriented GO nanosheets reduces the speed of permeation of all gases. The gas molecules, which pass through the perpendicularly oriented GO nanosheets significantly control the permeation behaviour of gas molecules. This might explain

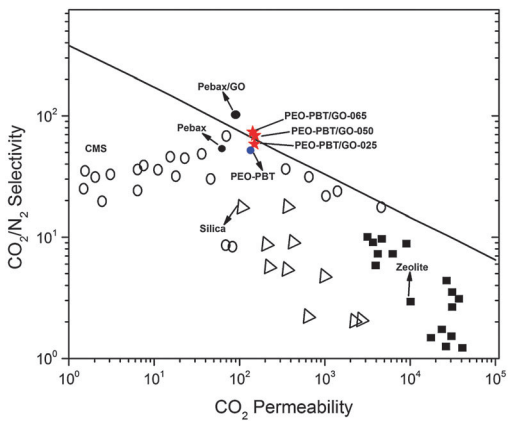


Fig. 4 Relationship between $CO_2$ permeability and $CO_2/N_2$ selectivity (Robeson plot) for PEO–PBT/GO membranes. The upper bound curve and gas separation data were obtained from ref. 17 and 21 (CMS – carbon molecular sieve).

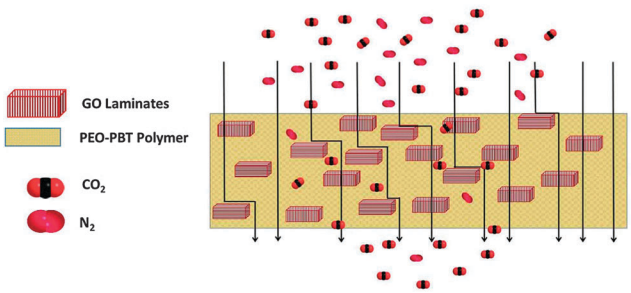


Fig. 5 Schematic illustration of possible GO nano-channels for gas transport in the PEO–PBT membrane.

Open Access Article. Published on 31 July 2015. Downloaded on 11/9/2025 4:47:51 AM.
This article is licensed under a Creative Commons Attribution-NonCommercial 3.0 Unported Licence.

why at high (0.5 wt%) loadings of GO nanosheets the permeability is reduced for all gases. The SEM images (Fig. S6, ESI†) of the top surface of the PEO–PBT/GO membrane shows a high GO aggregation for the 0.5 wt% GO PEO–PBT membrane. The AFM image (Fig. S7, ESI†) of the PEO–PBT/GO membrane further confirms the aggregation of GO in the membrane surfaces.

We demonstrated the preparation of defect-free thin film composite membranes by coating a PAN porous support membrane with the PEO–PBT/GO solution followed by solvent evaporation. Developing a defect-free thin film composite membrane with high gas permeability and high selectivity is a challenge. We succeeded in developing a defect-free thin film composite PEO–PBT/GO membrane by a simple dip-coating process, which can be up-scaled easily to produce commercial scale gas separation membranes. A 3 wt% PEO–PBT/GO solution was prepared by dissolving a copolymer in THF/DI water (80/20 w/w) and then a porous ultrafiltration PAN support membrane was dip-coated with the PEO–PBT/GO solution. Then, the membranes were dried at room temperature and their gas fluxes were measured. The gas flux and the selectivity are reported in Table S2 (ESI†). The selectivities of the thin film composite membranes were similar to those of the dense PEO–PBT/GO films. The gas permeation data prove the formation of defect free thin film PEO–PBT/GO composite membranes.

In summary, we have successfully prepared a PEO–PBT/GO mixed matrix membrane for the selective separation of $CO_2$. The PEO–PBT/GO membranes showed high $CO_2$ permeability and a $CO_2/N_2$ selectivity suitable for practical separation applications. The GO addition to the PEO–PBT membrane increased the $CO_2/N_2$ selectivity from 52 to 73, maintaining the same high permeability of a pristine PEO–PBT membrane. We also demonstrated the formation of defect-free thin film composite PEO–PBT/GO membranes by a simple dip coating procedure. The membrane formation by this method has a distinct advantage in terms of facile membrane fabrication for practical $CO_2$ capture applications.

## Notes and references

1 H. W. Kim, H. W. Yoon, S. M. Yoon, B. M. Yoo, B. K. Ahn, Y. H. Cho, H. J. Shin, H. Yang, U. Paik, S. Kwon, J. Y. Choi and H. B. Park, *Science*, 2013, **342**, 91.
2 Z. P. Smith and B. D. Freeman, *Angew. Chem., Int. Ed.*, 2014, **53**, 10286.
3 H. Li, Z. Song, X. Zhang, Y. Huang, S. Li, Y. Mao, H. J. Ploehn, Y. Bao and M. Yu, *Science*, 2013, **342**, 95.
4 G. Li, L. Shi, G. Zeng, M. Li, Y. Zhang and Y. Sun, *Chem. Commun.*, 2015, **51**, 7345.
5 R. K. Joshi, P. Carbone, F. C. Wang, V. G. Kravets, Y. Su, I. V. Grigorieva, H. A. Wu, A. K. Geim and R. R. Nair, *Science*, 2014, **343**, 752.
6 J. S. Bunch, S. S. Verbridge, J. S. Alden, A. M. Zande, J. M. Parpia, H. G. Craighead and P. L. McEuen, *Nano Lett.*, 2008, **8**, 2458.
7 D. R. Dreyer, S. Park, C. W. Bielawski and R. S. Ruoff, *Chem. Soc. Rev.*, 2010, **39**, 228.
8 R. R. Nair, H. A. Wu, P. N. Jayaram, I. V. Grigorieva and A. K. Geim, *Science*, 2012, **335**, 442.
9 H. Huang, Z. Song, N. Wei, L. Shi, Y. Mao, Y. Ying, L. Sun, Z. Xu and X. Peng, *Nat. Commun.*, 2013, **4**, 2979.
10 P. Sun, M. Zhu, K. Wang, M. Zhong, J. Wei, D. Wu, Z. Xu and H. Zhu, *ACS Nano*, 2013, **7**, 428.
11 Y. P. Tang, D. R. Paul and T. S. Chung, *J. Membr. Sci.*, 2014, **458**, 208.
12 W. Gao, G. Wu, M. T. Janicke, D. A. Cullen, R. Mukundan, J. K. Baldwin, E. L. Brosha, C. Galande, P. M. Ajayan, K. L. More, A. M. Dattelbaum and P. Zelenay, *Angew. Chem., Int. Ed.*, 2014, **53**, 3588.
13 H. W. Kim, H. W. Yoon, B. M. Yoo, J. S. Park, K. L. Gleason, B. D. Freeman and H. B. Park, *Chem. Commun.*, 2014, **50**, 13563.
14 L. Chen, L. Huang and J. Zhu, *Chem. Commun.*, 2014, **50**, 15944.
15 K. Huang, G. Liu, Y. Lou, Z. Dong, J. Shen and W. Jin, *Angew. Chem., Int. Ed.*, 2014, **53**, 6929.
16 D. A. Dikin, S. Stankovich, E. J. Zimney, R. D. Piner, G. H. Dommett, G. Evmenenko, S. T. Nguyen and R. S. Ruoff, *Nature*, 2007, **48**, 457.
17 L. M. Robeson, *J. Membr. Sci.*, 2008, **320**, 390.
18 D. Bastani, N. Esmaeili and M. Asadollahi, *J. Membr. Sci.*, 2013, **19**, 375.
19 T. S. Chung, L. Y. Jiang, Y. Li and S. Kulprathipanja, *Prog. Polym. Sci.*, 2007, **32**, 483.
20 T. Li, Y. Pan, K.-V. Peinemann and Z. Lai, *J. Membr. Sci.*, 2013, **425–426**, 235.
21 J. Shen, G. Liu, K. Huang, W. Jin, K.-R. Lee and N. Xu, *Angew. Chem., Int. Ed.*, 2014, **53**, 1.
22 X. Li, Y. Cheng, H. Zhang, S. Wang, Z. Jiang, R. Guo and H. Wu, *ACS Appl. Mater. Interfaces*, 2015, **7**, 5528.
23 T. Brinkmann, C. Naderipour, J. Pohlmann, J. Wind, T. Wolff, E. Esche, D. Mueller, G. Wozny and B. Hoting, *J. Membr. Sci.*, 2015, **489**, 237.
24 W. Yave, A. Car, S. S. Funari, S. P. Nunes and K.-V. Peinemann, *Macromolecules*, 2010, **43**, 326.
25 O. C. Compton, S. W. Cranford, K. W. Putz, Z. An, L. C. Brinson, M. J. Buehler and S. T. Nguyen, *ACS Nano*, 2012, **6**, 2008.
26 L. M. Malarda, M. A. Pimentaa, G. Dresselhaus and M. S. Dresselhaus, *Phys. Rep.*, 2009, **473**, 51.

 This journal is © The Royal Society of Chemistry 2015